Submitted: 01/14/19

Research Article

[1]McGill University, Montreal, QC, Canada
[2]Lamont-Doherty Earth Observatory, Columbia University, New York, USA

Keywords

Multi-year ice (MYI), First-year ice (FYI), Promotion, Demotion, Export

Email Correspondence

jamie.hart@mail.mcgill.ca

Jamie Hart[1], Bruno Tremblay[1,2], Charles Brunette[1], Carolina Dufour[1], Robert Newton[2]

Examining the Transition from a perennial to a seasonal sea ice cover in the Arctic Ocean: A Lagrangian Approach

Abstract

Background: Declining Arctic sea ice extent has been accompanied by a large loss in multiyear ice (MYI). The dynamic and thermodynamic processes which affect this transition include promotion of first year ice (FYI) to MYI, demotion (melting) of MYI to open water, and ice export through Fram Strait. In this study we quantify the relative importance of these three processes.

Methods: We use the Lagrangian Ice Tracking System which employs satellite-derived sea ice drift vectors combined with sea ice concentrations to find annual areas of promotion, demotion, and export.

Results: Over the satellite record (1989-2015), we quantify the total contributions to sea ice extent loss from promotion (+30 million km^2), demotion (-19.7 million km^2), and export of MYI (-18.6 million km^2). The result is a total net loss of 8.3 million km^2 of MYI. We find that all three processes are positively correlated with minimum sea ice extent and are increasing with rates of +0.165 million km^2/decade, -0.146 million km^2/decade, and -0.096 million km^2/decade for promotion, demotion, and export respectively. We also compute the negative ice growth feedback at 0.59 (with r^2=0.27). This indicates that ice pack recovers, on average, 59% of the MYI area lost to demotion/export through promotion of FYI the following winter.

Limitations: Uncertainties in the drift speed are compounded by the weekly temporal resolution of the model, which affects the resulting estimates of demotion and promotion area.

Conclusion: Demotion and export combined are increasing faster than promotion and represent a larger area contribution. This imbalance accounts for the observed loss of MYI area.

Introduction

Arctic sea ice extent has been declining rapidly over the satellite record. From 1979 to 2014, the September minimum sea ice extent has declined at a rate of -13.3% per decade (1). The reduced spatial coverage has been accompanied by a decrease in multi-year ice (MYI; 2,3,4,5), defined as ice that has survived through at least one melt season. In the mid-1980s, MYI constituted 75% of the total ice extent (3) but has fallen by more than 50% since the year 2000 (5). As first year ice (FYI) replaces MYI as the dominant ice type, the ice pack is generally thinner and shows reduced extent for a given summer melt (5).

Promotion of FYI to MYI and demotion of MYI to open water have critical implications for marine ecosystems. Plankton, nutrients and sediment are entrained into FYI as it forms and transported to the site where the ice melts. Promotion to MYI is important for the long-distance transport of these materials, e.g.: to the Central Arctic and other peripheral seas. Indeed, this transport results in the high productivity of some Arctic peripheral sea fisheries, such as the Barents Sea (6). Recently, changes in FYI and MYI distribution are altering this transport and endangering the ecosystem. This ecosystem is estimated to disappear within 20 years, the most rapid disappearance of an ecosystem associated with climate change yet recorded (7).

Demotion is not the only mechanism of MYI loss: export through the Fram Strait and subsequent melting also diminishes Arctic MYI area. The Fram Strait is the passage between Greenland and Svalbard. Fram Strait ice export is important for the Arctic sea ice budget, since about 10% of the total sea ice mass is exported through here annually (8). Ice export and import through other straits (Bering, Davis, Nares) are an order of magnitude smaller (9,10,11). Moreover, export rates through the Fram Strait are determined by the strength and position of the Transpolar Drift Stream (TDS) and can vary annually by up to 50% (12). On longer timescales, Fram Strait export is affected by atmospheric climate variations such as the North Atlantic Oscillation (NAO)/Arctic Oscillation (AO). During a positive NOA/AO, the pressure gradient across the Fram Strait increases, causing higher export (13).

When the Arctic system is perturbed by external climate forcings, various internal processes will react either by pushing the system back to equilibrium (negative feedback) or further away from its equilibrium (positive feedback). There are several positive feedbacks which amplify warming once open water and FYI are present. For example, the ice-albedo positive feedback, wherein warming decreases ice cover or increases melt-pond fraction, creating a surface with a lower albedo (reflectivity), which absorbs more solar energy, leading to more warming (14). Nevertheless, there are also negative feedbacks. For example, the ice-growth feedback, where open water or thinner ice cover both emit more radiation than colder thicker ice (thin ice conducts the ocean's heat), causing more heat loss, and therefore ice growth in the next year. Overall, the Arctic's positive feedback loops dominate and drive the transition from a large area of thick MYI towards thinner FYI and a seasonally ice-free Arctic (15,16).

The occurrence of an ice-free arctic summer is currently predicted to occur before the end of the 21st century (4). In 2007, results from the Coupled Model Intercomparison Project Phase 3 (CMIP3) reported in the United Nations Intergovernmental Panel on Climate Change (IPCC) Fourth Assessment Report (AR4) predicted nearly-ice free conditions in the year 2075. More recent estimates now predict occurrence of an ice-free Arctic in just a few decades, with many CMIP5 models showing essentially ice-free conditions by 2050 (17). There are still large uncertainties in these estimates due to uncertainties in the physics of climate models, future anthropogenic emissions, and natural climate variability. Indeed, natural climate variability alone creates uncertainties on the order of two decades (18). Therefore, understanding the processes of MYI loss is imperative to improving climate models' performance and decreasing uncertainty in the prediction of an ice-free Arctic summer.

In this study, we investigate the large loss of MYI in the Arctic Ocean, with the goal of quantifying the relative importance of the thermodynamic and dynamic processes causing this change, namely: demotion (melting) of MYI to open water, promotion of FYI to MYI, and export of MYI through the Fram Strait. We also map the areas of the Arctic where these processes predominantly occur. To accomplish this, we use the Lagrangian Ice Tracking System (19-20) forced with satellite-derived sea ice drift data together with observed sea ice concentration. The results from this study will help determine if the mechanisms responsible for the transition to a seasonal ice cover in current general circulation models (GCMs) are realistic. If not, it will help identify key processes that are not currently well-represented in GCMs and limit seasonal sea ice predictability.

Methods

I. Sea Ice Concentration

Sea ice concentration (SIC) is defined as the fraction of each grid cell covered by ice. Furthermore, the sea ice extent is the total area covered by the sea ice pack, with each grid cell requiring at least 15% SIC to be accepted as ice-covered. We justify this commonly-used threshold by the fact that concentration increases quickly from the edge of the pack ice inwards. We calculate the sea ice extent from the SIC data and the grid cell area. The SIC data comes from the National Oceanic and Atmospheric Administration (NOAA)/National Snow & Ice Data Center (NSIDC) Climate Data Record (CDR) Passive Microwave Sea Ice Concentration Version 3 (21), which provides daily and monthly SIC data. This information is provided on a polar stereographic grid with a 25 x 25 km Equal-Area Scalable Earth (EASE) grid spatial resolution (22). We produce weekly SIC averages interpolated on the EASE-Grid from 1980 to 2015. Note that in 1987 and 1988, due to maintenance issues, two periods of data were lost: 1987 weeks 28-31, and 1987 weeks 49-52 through 1988 weeks 1-2. The second period through the 87/88 winter could be set to the surrounding week's SIC, since SIC changes little over the winter in the central Arctic. However, the first period in the spring of 1987 is a time of large variability in sea ice: therefore, we simply exclude 1987 in our results.

II. Sea Ice Drift

Sea ice drift is the motion of sea ice due to wind, ocean currents, the Coriolis force, internal ice stress, and sea surface tilt. Only sea ice which is attached to the shore ("fast ice") does not drift. We use the NSIDC Polar Pathfinder (PPF) Daily 25 km EASE-Grid Sea Ice Motion Vectors, Version 3 (23), which provides daily, monthly, and weekly sea ice drift data on a 25 x 25 km EASE grid projection. The sea ice drift vectors are the product of an interpolation which combines input from four types of sources: buoys from the International Arctic Buoy Program (IABP), passive microwave sensors (AMSR-E, SMMR, SSM/I, SSMIS), visible and infrared radiometer channels (AVHRR), and free-drift estimate derived from NCEP/NCAR wind Reanalysis (23). When the aforementioned data is missing or unreliable, we use free drift estimates derived from NCEP/NCAR Reanalysis data. We use the weekly averaged sea ice drift vectors from 1980 to 2015.

III. Lagrangian Ice Tracking System (LITS)

Sea ice was advected (i.e. transported horizontally) using the Lagrangian Ice Tracking System (LITS) (19-20). This system takes an initial ice-covered tracer on the EASE grid and advects it in one-week increments using interpolated PPF weekly drift vectors from the start date to the end date. Through each advection step, LITS checks the SIC to make sure the tracer is still in an area covered by sea ice (we refer to this tracer as "active"). If the tracer melts (SIC drops below 15%), then LITS marks it as inactive and stops advection. The location error (i.e. the distance between the true buoy location and the trajectory estimated by LITS) yields a median and third quartile error of 7% and 16%, respectively, for typical Arctic Ocean sea ice drift speeds of 3-5 cm/s (20).

IV. Advection Protocol

We show a step-by-step example for the advection procedure from year 2014 to 2015 (Fig. 1). We start each year at the week of the minimum sea ice extent (SIE), which occurs at the end of the summer melt season, usually in September. According to our definition, all sea ice present at this time is MYI since it has survived the summer melt. The initial 2014 minimum sea ice pack is tagged inside of a mask which excludes the Canadian Arctic Archipelago (CAA, where no winter drifts are present) and everything south of the Fram Strait (Fig. 1a), with each tracer representing a 25 x 25 km grid cell. The boundary is then found using the MATLAB function *bwboundaries*, taking only the largest object found and excluding interior holes. The tracers are then advected in weekly increments until the time of the 2015 minimum sea ice extent (Fig. 1b). If a tracer melted early in the season (i.e. after March, at the very end of winter), its last position is recorded. This allows us to identify ice loss associated with the melt front early in the spring/summer season. Because of the dispersion of the tracers, the new boundary is less well-defined. In this case, we use the MATLAB function *alphaShape* to bound the advected area (Fig. 1c). The *alphaShape* boundary is considered the 2014 ice edge advected to September 2015 (Fig. 1d). Next, the 2015 observed minimum sea ice edge is found using *bwboundaries* as before and is overlaid on top of the 2014 advected edge (Fig. 1d). Finally, by subtracting the two boundaries, the areas of promotion and demotion are identified (Fig. 1e), indicating regions of FYI promotion and MYI demotion. Where the observed ice edge extends further south than the previous year advected ice edge, newly formed ice survived the 2015 summer melt: this ice corresponds to the promotion of FYI to MYI. Where the observed ice edge extends farther north than the advected ice edge, the existing MYI is lost through melting: this ice corresponds to the demotion of MYI to open water. Note that FYI promoted to MYI could be demoted (melt or export) on its second year of life.

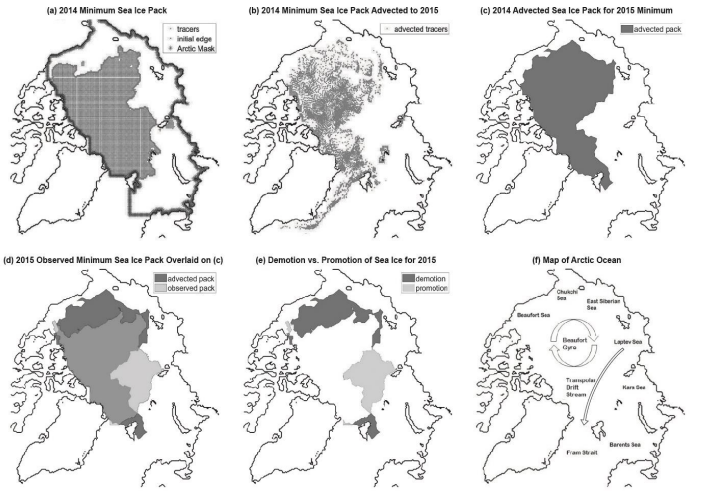

Fig. 1. (a) Initial position of tracers for 2014 pack. (b) Final position of tracers in (a) advected 1 year to September 2015. (c) Advected MYI pack from 2014 to 2015. (d) 2015 minimum pack overlaid on (c), where medium grey tone indicates region overlap. (e) Regions of promotion and demotion. (f) Arctic map listing peripheral seas/sea ice circulation features.

V. Fram Strait MYI Export

MYI is also lost by leaving the Arctic region (mask) through the Fram Strait, which is not properly accounted for by the method described above. We know that once this MYI crosses the Fram Strait, it will eventually be melted by the North Atlantic heat flux. Therefore, we count it as a loss outside the region. Hence, we need to calculate the transport of MYI across Fram Strait accurately. When the method described in section 2. IV is applied to the Fram Strait outside the mask, MYI loss is underestimated by almost 80% compared with other studies (8,12). We explain this by the North Atlantic heat influx continually melting parcels in the same location, and this overlapping of melted parcels resulting in a smaller computed area boundary compared to the actual area of MYI exported. As such, we require a different approach when addressing Fram Strait export. Instead, we count the number of tracers advected out the Fram Strait each year and multiply by the area of a grid cell (625 km^2). Since each of these tracers came from the Arctic Ocean and occupied an area of 25 x 25 km to

begin with, we have a direct way to calculate the loss of Arctic Ocean MYI area. Using our method, we find a MYI export over the 35-year period of 18.6 M km², or 547 000 km²/year. Our result is approximately 60% of the export computed by other studies who considered FYI and MYI (8,12). This is appropriate, since over the last 8 years the proportion of Fram Strait export that comes from MYI ranges from 64% to 90% of the total export, where the remaining percentage consists of FYI (24).

VI. Error analysis

We estimate LITS ice-drift track errors by comparing LITS, forced with PPF sea-ice drifts with buoy drift trajectories, which we consider to be error-free. The result is a median location error of 7% for typical Arctic sea ice drifts of 3-5 cm/sec (20). There is also an error in the areas of FYI promotion and MYI demotion associated with the temporal resolution of the model (one week). An upper bound error estimate for the error of tracers starting near the ice edge and drifting perpendicular to the ice edge towards open water can be written as $u_{ice} * \Delta t * L$ where Δt is 7 days and L is a typical synoptic length scale (500 km). Such a tracer would end its trajectory in open water and would be tagged as inactive for the next time step. As such, this error only applies to the demotion of MYI and always leads to an overestimate in MYI demotion area. For instance, an average ice drift speed of 4 or 10 cm/s in the central Arctic yields an upper bound error of approximately 12 or 30 thousand km².

Results and Discussion

I. Regions of Promotion and Demotion

We find two unique patterns for both promotion and demotion in the periods 1980-1999 and 2000-2015 (Fig. 2). We compare observations from the beginning of the satellite era (1980-1999) to the more recent period (2000-2015). In the pre-2000 (1980-1999), the regions of promotion and demotion are spread among the peripheral seas (Fig. 2a and 2b), whereas in the post-2000 (2000-2015), these regions are larger and extend poleward because of the increased drift speed (25, 26, Fig. 2c and 2d).

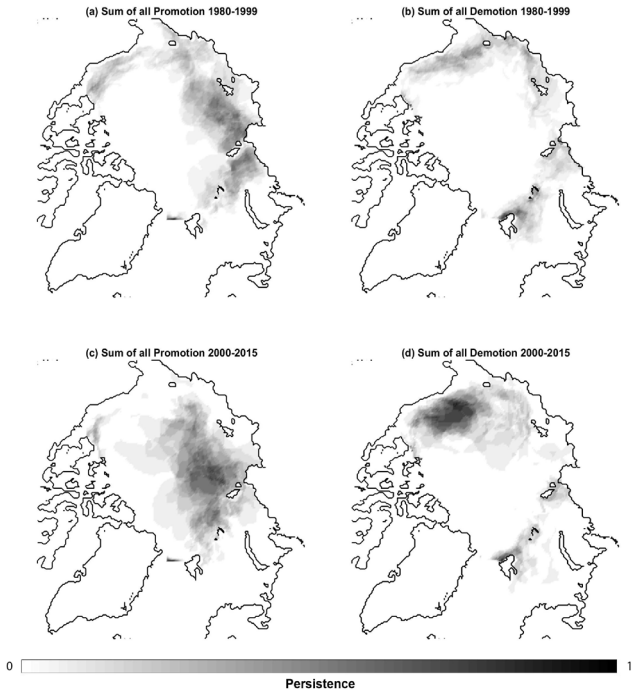

Fig. 2. Regions of (a,c) promotion and (b,d) demotion for (a,b) 1980-1999 and (d,c) 2000-2015. The grey gradient indicates persistence, which refers to the fraction of the given time period that a pixel experienced (a,c) FYI promotion or (b,d) MYI demotion.

In the earlier period, promotion is mainly located in the Laptev Sea extending into the Kara Sea, with smaller centres also along the shorelines in the East Siberian, Chukchi, Beaufort, and Northern Barents Seas (Fig. 2a). It is well documented that promotion occurs consistently in the Laptev Sea due to divergence from the coastline, giving it the name of sea ice factory (27). This region is the source of the Transpolar Drift Stream, which transports FYI from the Laptev sea to the central Arctic and Fram Strait (20). In the later period, this main promotion region increases in size and persistence (Fig. 2c), indicating a stronger transpolar drift stream (25,26).

In the earlier period, promotion is mainly located in the Laptev Sea extending into the Kara Sea, with smaller centres also along the shorelines in the East Siberian, Chukchi, Beaufort, and Northern Barents Seas (Fig. 2a). It is well documented that promotion occurs consistently in the Laptev Sea due to divergence from the coastline, giving it the name of sea ice factory (27). This region is the source of the Transpolar Drift Stream, which transports FYI from the Laptev sea to the central Arctic and Fram Strait (20). In the later period, this main promotion region increases in size and persistence (Fig. 2c), indicating a stronger transpolar drift stream (25,26).

In general, the transition from a perennial to a seasonal ice cover leads to a clear separation between centers of demotion and promotion. More specifically, promotion mainly occurs in the Eurasian Arctic, while demotion (of primarily Beaufort Sea MYI) is more prominent in the Pacific sector of the Arctic (Fig 2c and 2d). Although areas of promotion and demotion have become more segregated over time, we still find overlap in peripheral regions, most notably in the Central Arctic Ocean and East Siberian Sea. We also identify small areas of intersection along the Beaufort Sea, Laptev Sea, and around the islands in the Kara and Barents Seas.

II. Temporal Variability

We observe an approximate balance between promotion, demotion and export in the 80s and 90s, but an increasing trend in promotion as well as demotion and export since 2000 (Fig. 3). This pattern shift could be related to atmospheric changes in NAO/AO, a serious consideration which is left to future work. Over the 35-year period, the sum of all promotion is 30.0 million km², whereas the sum of all demotion is -19.7 million km², and the sum of all export is -18.6 million km². The net change in MYI area (i.e. promotion minus demotion minus export) for the entire period is -8.3 million km², which corresponds to -2.4 million km²/decade. In the later period (2000-2015) we calculate MYI loss at -5.5 million km², which is much higher than satellite-derived estimates of -2 million km² for 1999-2017 (5). Our very different approaches, lagrangian tracking andeulerian satellite field analysis, may explain this discrepancy. We find increasing trends in promotion (0.16 million km²/decade), demotion (-0.15 million km²/decade), and export (-0.096 million km²/decade), all beyond the 98% confidence level. This results in a trend for the net change in MYI of -0.08 million km²/decade, with a significance of 72%.

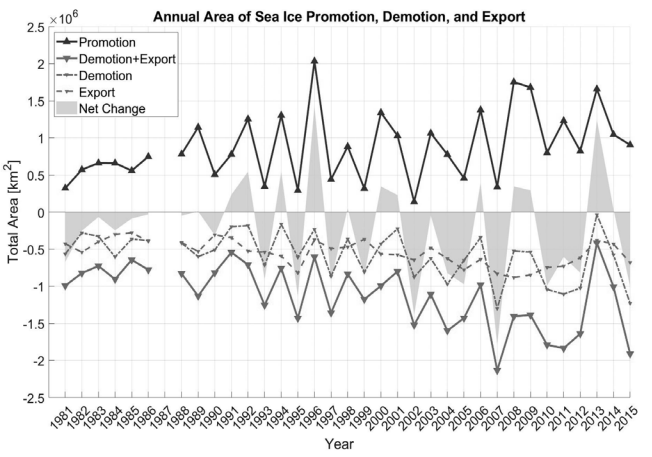

Fig. 3. Time series of sea ice area of FYI promotion (upward arrow), export (long dashed gray), MYI demotion (short dashed gray), and MYI demotion plus export (downward arrow) for time period 1981-2015. The lighter filled area represents the net change in sea ice area from year n-1 to year n (promotion - demotion - export).

III. Correlations

We further investigate the temporal variability of promotion, demotion, and export by examining the correlation of SIE minimum. We compute the annual correlation of detrended anomaly time series for promotion, demotion, and export against the same year minimum SIE. We find moderate positive correlations of 0.52, 0.51 and 0.30, respectively. Therefore, promotion and demotion serve as diagnostic variables for increasing sea ice loss. We attribute decreasing minimum sea ice extent to increasing rate of demotion and export. This will be further investigated.

IV. Negative Ice Growth Feedback

We analyze both positive and negative feedbacks using lagged cross-correlations between demotion, promotion, and export. The only significant correlation we find is the negative ice growth feedback, which is the tendency for a year of high demotion and export to be followed by a year of high promotion. To quantify the negative ice growth feedback, we investigate the relationship between MYI loss mechanisms (demotion and export) and the subsequent year's MYI growth mechanism (promotion). The best line fit between scatter plot of promotion in year *n+1* versus demotion and export in year *n* has a slope of 0.59 with an r-squared value of 0.27, indicating a moderate strength feedback (Fig. 4). This means that on average 59% of MYI demotion in a given year will be compensated by FYI promotion the following year.

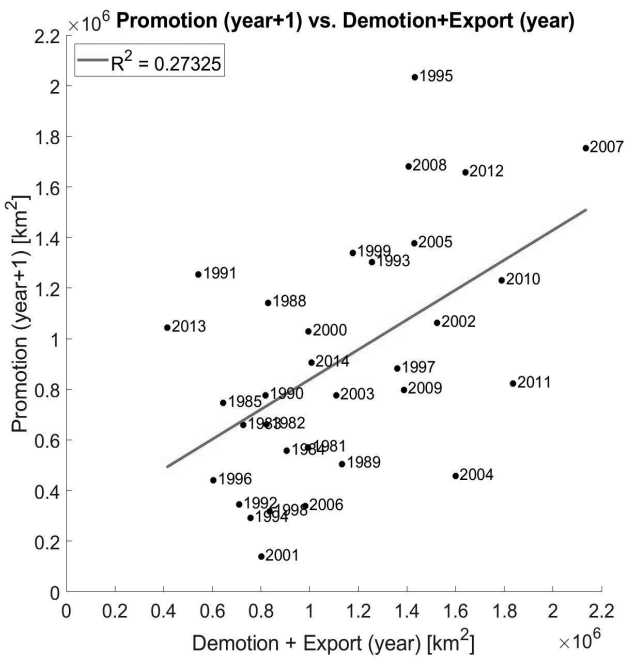

Fig. 4. Scatter plot of the total sea ice area of promotion in year *n+1* versus demotion + export for year *n*. The gray dotted line is a linear regression with an r^2 value of 27%. Years 1986, 1987, and 2015 cannot be calculated because of the missing 1987 data (see section 2. I) and the end of the dataset in 2015.

Given the feedback loops present in the perturbed Arctic system, we cannot assume any current trend to continue linearly. If the increase in FYI and decrease in MYI continue, the mechanisms of warming and ice loss may intensify and increase the rate exponentially.

Conclusion

In this study, we examine the mechanisms responsible for recent MYI loss in the Arctic. To do so, we use a Lagrangian approach to quantify promotion of FYI to MYI, demotion of MYI to open water, and export of MYI through the Fram Strait. Results show a change in both the MYI growth and loss in the Arctic. Since 1980, we estimate promotion of FYI to MYI (8.6 million km2/decade for a total of 30 million km²), demotion of MYI to open water (-5.6 million km²/decade for a total of -19.7 million km²), and export of MYI through the Fram Strait (-5.3 million km²/decade for a total of -18.6 million km²). The combined effect of demotion and export is a net MYI loss of -8.3 million km² over the period. This is in general agreement with satellite derived estimate of sea ice extent in the Arctic since the beginning of the satellite era in the late seventies. We find increasing trends for each process at +0.165 million km2/decade for promotion, -0.146 million km²/decade for demotion, and -0.096 million km²/decade for export. We document a correlation between high demotion and export years and subsequent high promotion years, corresponding to a negative ice growth feedback of 59%. We find that demotion and promotion are both positively correlated with minimum sea ice extent. We thus conclude that demotion is primarily responsible for the transition from perennial to seasonal ice pack. Future work will include considering potential biases in sea ice drift vectors and investigating to what extent they can cause under or over-estimation of demotion and promotion areas.

Acknowledgements

This work was supported by the Natural Sciences and Engineering Research Council's Undergraduate Student Research Award. We thank NOAA and NSIDC for the SIC data Climate Data Record (CDR), as well as NSIDC for the Polar Pathfinder sea ice drift data.

References

1. Serreze MC, Stroeve J. Arctic sea ice trends, variability and implications for seasonal ice forecasting. Phil. Trans. R. Soc. A. 2015 Jul 13;373(2045):20140159.

2. Comiso JC. A rapidly declining perennial sea ice cover in the Arctic. Geophysical Research Letters. 2002 Oct 18;29(20):17-1-17-4.

3. Maslanik J, Stroeve J, Fowler C, Emery W. Distribution and trends in Arctic sea ice age through spring 2011. Geophysical Research Letters. 2011 Jul 14;38(13).

4. Stroeve JC, Kattsov V, Barrett A, Serreze M, Pavlova T, Holland M, et al. Trends in Arctic sea ice extent from CMIP5, CMIP3 and observations. Geophysical Research Letters. 2012 Aug 28;39(16).

5. Kwok R. Arctic sea ice thickness, volume, and multiyear ice coverage: losses and coupled variability (1958–2018). Environmental Research Letters. 2018 Oct 12;13(10):105005.

6. Barber DG, Hop H, Mundy CJ, Else B, Dmitrenko IA, Tremblay JE, et al. Selected physical, biological and biogeochemical implications of a rapidly changing Arctic Marginal Ice Zone. Progress in Oceanography. 2015 Dec 1;139:122-50.

7. Fossheim M, Primicerio R, Johannesen E, Ingvaldsen RB, Aschan MM, Dolgov AV. Recent warming leads to a rapid borealization of fish communities in the Arctic. Nature Climate Change. 2015 May 18;5(7):673-7.

8. Smedsrud LH, Halvorsen MH, Stroeve JC, Zhang R, Kloster K. Fram Strait sea ice export variability and September Arctic sea ice extent over the last 80 years. The Cryosphere. 2017 Jan 13;11(1):65-79.

9. Kwok R. Baffin Bay ice drift and export: 2002–2007. Geophysical Research Letters. 2007 Oct 2;34(19).

10. Kwok R, Cunningham GF, Wensnahan M, Rigor I, Zwally HJ, Yi D. Thinning and volume loss of the Arctic Ocean sea ice cover: 2003–2008. Journal of Geophysical Research: Oceans. 2009 Jul 7;114(C7).

11. Babb DG, Galley RJ, Asplin MG, Lukovich JV, Barber DG. Multiyear sea ice export through the Bering Strait during winter 2011–2012. Journal of Geophysical Research: Oceans. 2013 Oct 1;118(10):5489-503.

12. Kwok R, Cunningham GF, Pang SS. Fram Strait sea ice outflow. Journal of Geophysical Research: Oceans. 2004 Jan 6;109(C1).

13. Kwok R, Rothrock DA. Variability of Fram Strait ice flux and North Atlantic oscillation. Journal of Geophysical Research: Oceans. 1999 Mar 15;104(C3):5177-89.

14. Curry JA, Schramm JL, Ebert EE. Sea ice-albedo climate feedback mechanism. Journal of Climate. 1995 Feb 1;8(2):240-7.

15. Auclair G, Tremblay LB. The Role of Ocean Heat Transport in Rapid Sea Ice Declines in the Community Earth System Model Large Ensemble. Journal of Geophysical Research: Oceans. 2018 Nov 29;123(12):8941-57.

16. Holland MM, Bitz CM, Tremblay B. Future abrupt reductions in the summer Arctic sea ice. Geophysical research letters. 2006 Dec 12;33(23).

17. Overland JE, Wang M. When will the summer Arctic be nearly sea ice free?. Geophysical Research Letters. 2013 May 28;40(10):2097-101.

18. Jahn A, Kay JE, Holland MM, Hall DM. How predictable is the timing of a summer ice-free Arctic?. Geophysical Research Letters. 2016 Sep 16;43(17):9113-20.

19. Williams J, Tremblay B, Newton R, Allard R. Dynamic preconditioning of the minimum September sea-ice extent. Journal of Climate. 2016 Aug 3;29(16):5879-91.

20. DeRepentigny P, Tremblay LB, Newton R, Pfirman S. Patterns of sea ice retreat in the transition to a seasonally ice-free Arctic. Journal of Climate. 2016 Sep 29;29(19):6993-7008.

21. Meier W, Fetterer F, Savoie MH, Mallory S, Duerr R, Stroeve JC. NOAA/NSIDC Climate Data Record of Passive Microwave Sea Ice Concentration, Version 3. NSIDC: National Snow and Ice Data Center: Boulder, Colorado USA 2017 [cited 12 Feb 2019]. Available from: https://nsidc.org/data/nsidc-0116

22. Peng G, Meier WN, Scott DJ, Savoie MH. A long-term and reproducible passive microwave sea ice concentration data record for climate studies and monitoring. Earth System Science Data. 2013 Oct 15;5(2):311-8.

23. Tschudi M, Fowler C, Maslanik J, Stewart S, Meier W. Polar Pathfinder Daily 25 km EASE-Grid Sea Ice Motion Vectors, Version 3. NASA National Snow and Ice Data Center Distributed Active Archive Center: Boulder, Colorado USA 2016 [cited 12 Feb 2019]. Available from: https://nsidc.org/data/G02202

24. Ricker R, Girard-Ardhuin F, Krumpen T, Lique C. Satellite-derived sea ice export and its impact on Arctic ice mass balance. The Cryosphere. 2018 Sep 25;12(9):3017-32.

25. Kwok R, Spreen G, Pang S. Arctic sea ice circulation and drift speed: Decadal trends and ocean currents. Journal of Geophysical Research: Oceans. 2013 Apr 9;118(5):2408-25.

26. Rampal P, Weiss J, Marsan D. Positive trend in the mean speed and deformation rate of Arctic sea ice, 1979–2007. Journal of Geophysical Research: Oceans. 2009 May 14;114(C5).

27. Reimnitz E, Dethleff D, Nürnberg D. Contrasts in Arctic shelf sea-ice regimes and some implications: Beaufort Sea versus Laptev Sea. Marine Geology. 1994 Jul 1;119(3-4):215-25.

28. Onarheim IH, Eldevik T, Smedsrud LH, Stroeve JC. Seasonal and Regional Manifestation of Arctic Sea Ice Loss. Journal of Climate. 2018 Jun 15;31(12):4917-32.

29. Kwok R, Cunningham GF. Contribution of melt in the Beaufort Sea to the decline in Arctic multiyear sea ice coverage: 1993–2009. Geophysical Research Letters. 2010 Oct 1;37(20).